https://doi.org/10.5194/esd-2021-27
Preprint. Discussion started: 1 July 2021

Earth System Dynamics
Discussions
Open Access
EGU

Title: **Quantifying memory and persistence in the atmosphere–land/ocean carbon system**

Authors: **Matthias Jonas[1*],**
Rostyslav Bun[2,3],
Iryna Ryzha[2] &
Piotr Żebrowski[1]

[1]Advancing Systems Analysis Program, International Institute for Applied Systems Analysis, 2361, Laxenburg, Austria. [2]Department of Applied Mathematics, Lviv Polytechnic National University, 79013, Lviv, Ukraine. [3]Department of Transport and Computer Sciences, WSB University, 41300, Dąbrowa Górnicza, Poland. [*]email: jonas@iiasa.ac.at

Keywords: Global carbon cycle, global atmosphere–land/ocean system, atmospheric CO_2 emissions, stress-strain model, Maxwell body, memory, persistence

https://doi.org/10.5194/esd-2021-27
Preprint. Discussion started: 1 July 2021

Earth System Dynamics
Discussions

Abstract

Here we interpret carbon dioxide (CO_2) emissions from fossil fuel burning and land use as a global stress-strain experiment. We use the idea of a Maxwell body consisting of elastic and damping (viscous) elements to reflect the overall behaviour of the atmosphere–land/ocean system in response to the continued increase of CO_2 emissions between 1850 and 2015. From the standpoint of a global observer, we see that as a consequence of the increase, the CO_2 concentration in the atmosphere increases (rather quickly). Concomitantly, the atmosphere warms and expands, while part of the carbon is locked away (rather slowly) in land and oceans, likewise under the influence of global warming.

It is not known how reversible and how much out of sync the latter process is in relation to the former. All we know is that the slower process remembers the influence of the faster one which runs ahead. Here we ask three (nontrivial) questions: (1) Can this global-scale memory—Earth's memory—be quantified? (2) Is Earth's memory a buffer which is negligently exploited; and in the case that it is even a limited buffer, what is the degree of exploitation? And (3) does Earth's memory allow its persistence (path dependency) to be quantified? To the best of our knowledge, the answers to these questions are pending.

We go beyond textbook knowledge by introducing three parameters that characterise the system: delay time, memory, and persistence. The three parameters depend, ceteris paribus, solely on the system's characteristic viscoelastic behaviour and allow deeper insights into that system. We find that since 1850, the atmosphere–land/ocean system has been trapped progressively in terms of persistence (i.e., it will become progressively more difficult to strain-relax the system), while its ability to build up memory has been reduced. The ability of a system to build up memory effectively can be understood as its ability to respond still

https://doi.org/10.5194/esd-2021-27
Preprint. Discussion started: 1 July 2021

within its natural regime; or, if the build-up of memory is limited, as a measure for system failures globally in the future. Approximately 60% of Earth's memory had already been exploited by humankind prior to 1959. We expect system failures globally well before 2050 if the current trend in emissions is not reversed immediately and sustainably.

https://doi.org/10.5194/esd-2021-27
Preprint. Discussion started: 1 July 2021

1. Motivation

Over the last century anthropogenic pressure on Earth became increasingly noticeable. Human activities turned out to be so pervasive and profound that the very life support system upon which humans depend is threatened (Steffen et al., 2004, 2015). The increase of emissions of greenhouse gases into the atmosphere is only one of several serious global threats and their reduction is in the center of international agreements (Steffen et al., 2015; United Nations, 2015a;b).

Here we intend to further the understanding of the planetary burden caused by global warming and the effect of the continued increase of GHG emissions from a new, a rheological perspective. We focus on carbon (CO_2) emissions from fossil fuel burning and land use between 1959 and 2015 (with the increase between 1850 and 1958 serving as upstream emissions).[5] From the standpoint of a global observer, we see that as a consequence of the increase, the CO_2 concentration in the atmosphere increases (rather quickly). Concomitantly, the atmosphere warms (here combining the effect of tropospheric warming and stratospheric cooling) and expands (by approximately 15–20 m in the troposphere per decade since 1990), while part of the carbon is locked away (rather slowly) in land and oceans, likewise under the influence of global warming (Global Carbon Project, 2019; Lackner et al., 2011; Philipona et al., 2018; Steiner et al., 2011; Steiner et al., 2020).

It is not known how reversible and how much out of sync the latter process is in relation to the former (Boucher et al., 2012; Dusza et al., 2020; Garbe et al., 2020; Schwinger and Tjiputra, 2018; Smith, 2012). All we know is that the slower process remembers the influence of the faster one which runs ahead. Here we ask three (nontrivial) questions: (1) Can this global-scale memory—Earth's memory—be quantified? (2) Is Earth's memory a buffer

https://doi.org/10.5194/esd-2021-27
Preprint. Discussion started: 1 July 2021

Earth System Dynamics
Discussions

which is negligently exploited; and in the case that it is even a limited buffer, what is the degree of exploitation? And (3) does Earth's memory allow its persistence (path dependency) to be quantified? To the best of our knowledge, the answers to these questions are pending.

To get a grip on Earth's memory, we focus on the slow-to-fast temporal offset inherent in the atmosphere–land/ocean system, while preferring an approach which is "as simple as possible but no simpler"; i.e. here, which does not come at the cost of complexity. To this end, it is sufficient to resolve subsystems as a whole and to perceive their physical reaction in response to the increase in atmospheric CO_2 concentrations as a combined one (i.e., including effects such as that of global warming). We refer to the subsystems' temporally disjunct reactions hereafter as the expansion of the atmosphere by volume and the sequestration of carbon by sinks. Under optimal conditions (referring to the long-term stability of the temporal offset), the temporal-offset view even suggests that we can refrain from disentangling the exchange of both thermal energy and carbon throughout the atmosphere–land/ocean system, as it is done in climate-carbon models ranging from simple to complex (Flato et al., 2013; Harman and Trudinger, 2014). The additional degree of simplicity will prove an advantage in advancing our understanding of the temporal offset in terms of memory and persistence.

In view of the aforementioned questions, we chose a rheological stress-strain (σ-ε) model (Roylance, 2001; TU Delft, 2021); here a Maxwell body (MB) consisting of an elastic element (its constant, traditionally denoted E [Young's modulus], is replaced by the compression modulus K) and a damping (viscous) element (the damping constant is denoted D), to capture the stress-strain behaviour of the global atmosphere–land/ocean system (Fig. 1) and to simulate how humankind propelled that global-scale experiment historically.

https://doi.org/10.5194/esd-2021-27
Preprint. Discussion started: 1 July 2021

Earth System Dynamics
Discussions

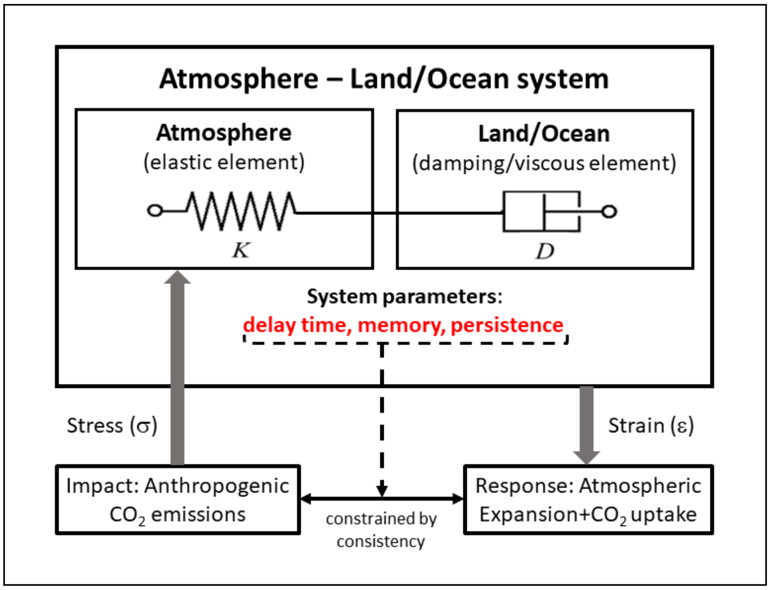

Fig. 1: Rheological model to capture the stress–strain behavior of the global atmosphere–land/ocean system as a Maxwell body, consisting of elastic (atmosphere) and damping/viscous (land/ocean) elements. The stress–strain behaviour is adjusted until consistency is achieved (see text).

In practice, rheology is principally concerned with extending continuum mechanics to characterise the flow of materials that exhibit a combination of elastic, viscous, and plastic behaviour by properly combining elasticity and (Newtonian) fluid mechanics. Limits (e.g., viscosity limits) exist beyond which basic rheological models are recommended to be refined. However, these limits are fluent, and basic rheological models also produce useful results beyond these limits (Mezger, 2006; TU Delft, 2021).

Depending on whether the strain (ε) or the stress (σ) is known (in addition to the compression and damping characteristics K and D), the stress-strain equation describing a MB can be applied in a stress-explicit form

https://doi.org/10.5194/esd-2021-27
Preprint. Discussion started: 1 July 2021

Earth System Dynamics
Discussions

$$\boldsymbol{\sigma(t) = \sigma(0)\, exp\left(-\frac{K}{D} t\right) + K \int_0^t \dot{\varepsilon}(\tau)\, exp\left(\frac{K}{D}(\tau - t)\right) d\tau} \tag{1a}$$

or in a strain-explicit form

$$\boldsymbol{\varepsilon(t) = \varepsilon(0) + \frac{1}{K}[\sigma(t) - \sigma(0)] + \frac{1}{D}\int_0^t \sigma(\tau)\, d\tau,} \tag{1b}$$

with $\sigma(0)$ and $\varepsilon(0)$ denoting initial conditions and a dot the derivative by time (Roylance, 2001; Bertram and Glüge, 2015).

For an observer it is the overall strain response of the atmosphere–land/ocean system (expansion of the atmosphere by volume and uptake of CO_2 by sinks) that is unknown. However, since atmospheric CO_2 concentrations have been observed to increase exponentially (quasi continuously), the strain can be expected to be exponential or close to exponential. In addition, we provide independent estimates of the likewise unknown compression and damping characteristics of the MB. This a priori knowledge allows equations (1a) and (1b) to be used stepwise in combination to narrow down our initial estimate of the K/D ratio, in particular. More accurate knowledge of this ratio is needed when we go beyond textbook knowledge by distilling three parameters—delay time (reflecting the temporal offset mentioned above), memory, and persistence—from the stress-explicit equation. The three parameters depend, ceteris paribus, solely on the system's characteristic K/D ratio and allow deeper insights into that system. We see the atmosphere–land/ocean system as being trapped progressively over time in terms of persistence. Given its reduced ability to build up memory, we expect system failures globally well before 2050 if the current trend in emissions is not reversed immediately and sustainably.

There exists a wide range of other approaches which aim at exploring memory and persistence in Earth systems data, typically with the focus on individual Earth subsystems or processes (e.g., atmospheric temperature or carbon dioxide emissions). So far, applied

https://doi.org/10.5194/esd-2021-27
Preprint. Discussion started: 1 July 2021

Earth System Dynamics
Discussions

approaches are mainly based on classical time-series and time-space analyses to uncover the memory or causal patterns contained in observational data (Barros et al., 2016; Belbute and Pereira, 2017; Caballero et al., 2002; Franzke, 2010; Lüdecke et al., 2013). However, these approaches come with well-known limitations which can all be attributed, directly or indirectly, to the issue of forecasting (more precisely, the conditions placed on the data to enable forecasting) or are not based on physics (Aghabozorgi et al., 2015; Darlington, 1996; Darlington and Hayes, 2016). By way of contrast, we do not forecast. We perpetuate long-term historical conditions which, in turn, allows the delay time in the atmosphere–land/ocean system to be expressed analytically in terms of memory and persistence.

Rheological approaches are common in Earth systems modeling as well. Typically, they are applied to mimic the long(er)-term behaviour of Earth subsystems, e.g. its mantle viscosity which is crucial for interpreting glacial uplift resulting from changes in planetary ice sheet loads (Müller, 1986; Whitehouse et al. (2019); Yuen et al., 1986). Yet, to the best of our knowledge, a rheological approach to unravel the memory-persistence behaviour of the global atmosphere–land/ocean system in response to the long-lasting increase in atmospheric CO_2 emissions had not been applied before.

We describe our rheological model (MB) approach in detail in Section 2, while we provide an overview of the applied data and conversion factors in Section 3. In Section 4 we describe how we derive first-order estimates of the main characteristics of the atmosphere–land/ocean system (in terms of the MB's K and D characteristics) by using available knowledge. Although uncertain, these estimates come useful in Section 5 where we apply the aforementioned stress and strain explicit equations to quantify delay time, memory, and

Earth System Dynamics Discussions

persistence of the atmosphere–land/ocean system. We conclude by taking account of our main findings in Section 6.

2. Method

We assume that we know the order of magnitude of both the K/D ratio characteristic of the atmosphere–land/ocean system and the rate of change in the strain ε given by $\dot{\varepsilon}(t) = \alpha\, exp(\alpha t)$ with the exponential growth factor $\alpha > 0$. These first-order estimates permit equations (1a) and (1b) to be used stepwise in combination:

Equation (1a): We vary both K/D and α to reproduce the known stress σ given by the CO_2 emissions from fossil fuel burning (fairly well known) and land use (less known) (Global Carbon Project, 2019).

Equation (1b): We insert both the fine-tuned K/D ratio and the known stress σ to compute the strain ε and check its derivative by time.

We consider this procedure a check of consistency, not a proof of concept.

Delay time, memory, and persistence are characteristic of the MB and are defined independently of initial conditions. Thus, we rewrite equation (1a) for $\sigma(0) = 0$, which results in

$$\sigma(t) = \frac{D}{\beta}\dot{\varepsilon}(t)\left(1 - q_\beta^t\right) \tag{2a}$$

(see Supplementary Information 1), where $\beta = 1 + \frac{D}{K}\alpha$ and $q_\beta^t = exp\left(-\frac{K}{D}\beta t\right)$. The term $\frac{D}{K\beta}$ represents a time characteristic of the MB under (here) exponential strain (i.e., of the MB that responds to the stress acting upon it), whereas $\frac{D}{K}$ is the relaxation time of the MB (i.e., of the MB that relaxes unhindered after the stress causing that strain has vanished, or that responds to strain held constant over time; also known as the relaxation test (Bertram and Glüge,

https://doi.org/10.5194/esd-2021-27
Preprint. Discussion started: 1 July 2021

2015). However, to ensure that exponents still come in units of 1 after we split them up, we introduce the dimensionless time $n = \frac{t}{\Delta t}$ globally (which will be discretised in the sequel when we refer to a temporal resolution of 1 year and set $\Delta t = 1y$), such that, for example, $q^t = exp\left(-\frac{K}{D}\Delta t\right)^n$.

To understand the systemic nature of the MB, we explore here its stress dependence on $q = exp\left(-\frac{K}{D}\Delta t\right)$, which contains the ratio of K and D, the two characteristic parameters of the MB, by way of derivation by q (while α is held constant). To this end, we transform equation (2a) further to

$$\sigma_D(q,t) := \frac{1}{D}\sigma(t) = \frac{1}{D}\sigma(n) =: \sigma_D(q,n) \tag{2b}$$

and execute $\frac{\partial}{\partial q}\sigma_D(q,n)$, the derivation by q of the system's rate of change σ_D (which is given in units of y^{-1}). Doing so allows (what we call) delay time T to be distilled (see Supplementary Information 2). It is defined as

$$T(q,n) := \frac{q_\beta}{S_n}\frac{\partial S_n}{\partial q_\beta} = -\frac{q_\beta^n}{1-q_\beta^n}n + \frac{q_\beta}{1-q_\beta}, \tag{3}$$

where $q_\beta = q_\alpha q$, $q_\alpha = exp(-\alpha\Delta t)$, and $S_n = S(q,n) = \frac{1-q_\beta^n}{1-q_\beta}$. The delay time behaves asymptotically for increasing n and approaches $T_\infty = \lim_{n\to\infty} T = \frac{q_\beta}{1-q_\beta}$. We further define

$$M := S(q,n) \tag{4}$$

with $M_\infty := \frac{1}{1-q_\beta}$ and

$$P := T(q,n)^{-1} \tag{5}$$

with $P_\infty := \frac{1}{T_\infty} = \frac{1-q_\beta}{q_\beta}$ as the MB's characteristic memory and persistence, respectively. As is commonly done, we keep the list of independent parameters minimal. (We only allow K and D [i.e., q] in addition to n; see equations [2b] and [3]–[5], in particular.)

https://doi.org/10.5194/esd-2021-27
Preprint. Discussion started: 1 July 2021

T as given by equation (3) is not simply characteristic of the MB described by equation (2); it can be shown to appear as delay time in the argument of any function dependent on current and previous times, with a weighting decreasing exponentially backward in time (see Supplementary Information 3). Equation (4) reflects the history the MB was exposed to systemically prior to current time n (during which α was constant; see Supplementary Information 4). Equation (5) can be shortened to $T \cdot P = 1$. If we assume that q can be changed in retrospect at $n = 0$, this equation tells us that if T —that is, ΔM per Δq (or, likewise, $\Delta M/M$ per $\Delta q/q$; see the first part of equation [3])—is small, P is great because the change in the system's characteristics (contained in q) hardly influences the MB's past, with the consequence that the past exhibits a great path dependency, and vice versa.

An additional quantity to monitor is $ln(M \cdot P)$, which approaches $\lambda_\beta = \lambda \cdot \beta$ for increasing n with $\lambda = \frac{K}{D}\Delta t$ the characteristic rate of change in the MB. The ratio $\lambda/ln(M \cdot P) \cdot$ allows monitoring of how much the system's natural rate of change is exceeded as a consequence of the continued increase in stress (see Supplementary Information 5).

3. Data and Conversion Factors

A detailed overview of the carbon data and conversion factors used in this paper is given in Supplementary Information 6. The data pertain to atmosphere, land, and oceans and are given by source and time range and are also described briefly. The context within which they are used is revealed in each of the following sections.

4. Independent Estimates of *D* and *K*

https://doi.org/10.5194/esd-2021-27
Preprint. Discussion started: 1 July 2021

Earth System Dynamics
Discussions

In this section we provide independent estimates of the damping and compression characteristics of the atmosphere–land/ocean system, with D_L and D_O denoting the damping constants assigned to land and oceans, respectively, and K denoting the compression modulus assigned to the atmosphere. We capture the characteristics' right order of magnitude only—which can be done on physical grounds by evaluating the combined (net) strain response of each subsystem on grounds of increasing CO_2 concentrations in the atmosphere. These first-order estimates are adequate as they allow sufficient flexibility for Section 5, where we narrow down our initial estimates by using equations (1a) and (1b) stepwise in combination to achieve consistency.

4.1 Estimating the Damping Constant D_L

Increasing concentrations of CO_2 in the atmosphere trigger the uptake of carbon by the terrestrial biosphere. The intricacies of this process, including potential (positive and negative) feedback processes, are widely discussed (Dusza et al., 2020; Smith, 2012; Heimann and Reichstein, 2008). The crucial question is how we have observed the process of carbon uptake by the terrestrial biosphere taking place in the past. Compared to the reaction of the atmosphere to global warming (an expansion of the atmosphere by volume), we consider this process to be long(er) term in nature and perceive it as a Newton-like (damping) element.

Biospheric carbon uptake is described by the biotic growth factor

$$\beta_b = \frac{\Delta NPP/NPP}{\Delta CO_2/CO_2}, \qquad (6)$$

which is used to approximate the fractional increase in net primary production (NPP) per unit increase in atmospheric CO_2 concentration (Amthor and Koch, 1996; Wullschleger et al., 1995). Here we make use of the model-derived NPP time series (1900–2016) provided by

https://doi.org/10.5194/esd-2021-27
Preprint. Discussion started: 1 July 2021

Earth System Dynamics
Discussions

O'Sullivan et al. (2019) to calculate β_b (O'Sullivan et al., 2019). To understand the uncertainty range underlying β_b, we use the photosynthetic beta factor

$$\beta_{Ph} = CO_2 L = \left(\frac{dPh}{Ph}\right)\left(\frac{CO_2}{dCO_2}\right), \quad (7)$$

where L is the so-called leaf-level factor denoting the relative leaf photosynthetic response to a 1 ppmv change in the atmospheric concentration of CO_2, where

$$L_1 \leq L = f(CO_2) \leq L_2, \quad (8)$$

and Ph is the global photosynthetic carbon influx for 1959–2018. Equation (7) is similar to equation (6). In equation (6) β_b represents biomass production changes in response to CO_2 changes, whereas in equation (7) β_{Ph} describes photosynthesis changes in response to CO_2 changes (Luo and Mooney, 1996).

L can be shown to be independent of plant characteristics, light, and the nutrient environment and to vary little by geographic location or canopy position. Thus, L is virtually a constant across ecosystems and a function of time-associated changes in atmospheric CO_2 only (Luo and Mooney, 1996).

We use equation (7) to test whether β_b falls in between the quantifiable photosynthetic limits L_1 (photosynthesis limited by electron transport) and L_2 (photosynthesis limited by rubisco activity). Fig. 2 shows the biotic growth factors from O'Sullivan et al. that consider changes in NPP due to the combined effect of CO_2 fertilisation, nitrogen deposition, climate change, and carbon–nitrogen synergy (β_{NPP_comb}) and due to CO_2 fertilisation (β_{NPP_CO2}) only. For 1960–2016, β_{NPP_comb} falls in between L_1 and L_2, closer to L_1 than to L_2, whereas β_{NPP_CO2} falls even below the lower L_1 limit.

https://doi.org/10.5194/esd-2021-27
Preprint. Discussion started: 1 July 2021

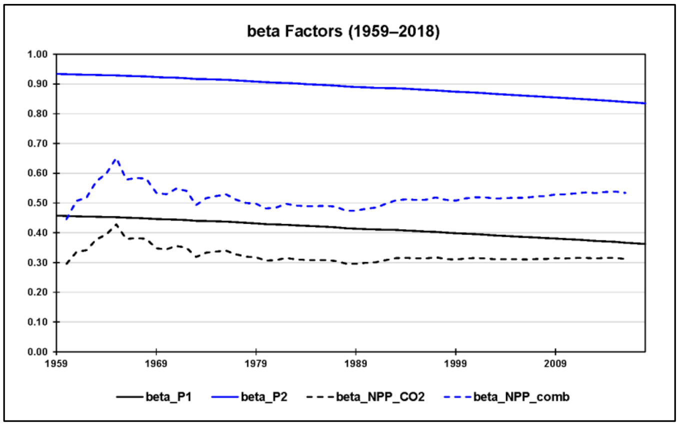

Fig. 2: Using the lower (β_1) and upper (β_2) limits of the photosynthetic beta factor to test the range of the biotic growth factor (β_b) for 1960–2016. The biotic growth factor is derived with the help of modelled net primary production (NPP) values provided by CO_2 fertilisation, nitrogen deposition, climate change, and carbon–nitrogen synergy. β_{NPP_CO2} refers to O'Sullivan et al. (2019),[35] who consider the change in NPP due to CO_2 fertilisation only, and β_{NPP_comb} refers to the change in NPP due to the combined effect.

Rewriting equation (7) in the form

$$\frac{\Delta Ph_i}{Ph} = L_i \Delta CO_2 \quad (i = 1,2) \tag{9}$$

with $Ph = 120 PgCy^{-1}$ indicating that the additional amount of annual relative photosynthetic carbon influx, stimulated by a yearly increase in atmospheric CO_2 concentration, can be estimated by L_i, or the sequence of L_i if ΔCO_2 spans multiple years (see Supplementary Information 7 and Supplementary Data 1). Plotting $\Delta Ph_i / Ph$ against time allows lower and upper slopes (rates of strain)

$$\frac{d}{dt}\left(\frac{\Delta Ph_1}{Ph}\right) \approx 0.0019 y^{-1} \text{ and } \frac{d}{dt}\left(\frac{\Delta Ph_2}{Ph}\right) = 0.0041 y^{-1} \tag{10a,b}$$

https://doi.org/10.5194/esd-2021-27
Preprint. Discussion started: 1 July 2021

to be derived for 1959–2018. A linear fit works well in either case. The cumulative increase in atmospheric CO_2 concentration since 1959, $\Delta CO_2 = CO_2(t) - CO_2(1959)$, exhibits a moderate exponential (close to linear) trend. Thus, plotting annual changes in CO_2, normalised on the aforementioned rates of strain, versus time allows the remaining (moderate) trends to be interpreted alternatively, namely, as average photosynthetic damping constants with appropriate uncertainty given by half the maximal range (see Fig. 3 and Supplementary Data 1)

$$D_1 \approx (815 \pm 433)ppmvy = (83 \pm 44)Pay = (2606 \pm 1383)10^6 Pas \qquad (11a)$$

$$D_2 \approx (378 \pm 201)ppmvy = (38 \pm 20)Pay = (1207 \pm 641)10^6 Pas \qquad (11b)$$

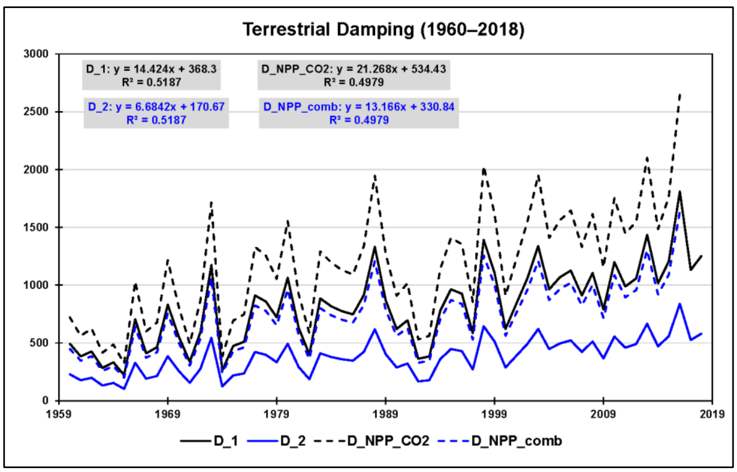

Fig. 3: Terrestrial carbon uptake perceived as damping (in ppmv y) based on the limits of leaf photosynthesis (1960–2018: D_1) and D_2) and on model-derived changes in net primary production (NPP; 1960–2016) due to both the combined effect of CO_2 fertilisation, nitrogen deposition, climate change, and carbon–nitrogen synergy (D_{NPP_comb}) and CO_2 fertilisation only (D_{NPP_CO2}). The linear trends of the four damping series are shown at the top. These are used to interpret damping as constants with appropriate uncertainty (given by half the maximal range).

https://doi.org/10.5194/esd-2021-27
Preprint. Discussion started: 1 July 2021

Repeating the same procedure for 1959–2016 with O'Sullivan et al.'s model-derived NPP values considering the change in NPP due to CO_2 fertilisation as well as the total change in NPP, we find

$$\frac{d}{dt}\left(\frac{\Delta NPP}{NPP}\right)_{CO2} \approx 0.0013y^{-1} \text{ and } \frac{d}{dt}\left(\frac{\Delta NPP}{NPP}\right)_{comb} = 0.0021y^{-1} \quad (12a,b)$$

(linear fits still work well); and consequently

$$D_{CO2} \approx (1172 \pm 617)ppmvy = (119 \pm 62)Pay = (3746 \pm 1971)10^6 Pas. \quad (13a)$$

$$D_{comb} \approx (726 \pm 382)ppmvy = (74 \pm 39)Pay = (2319 \pm 1220)10^6 Pas. \quad (13b)$$

As before, these estimates are closer to the lower leaf-level factor (higher photosynthetic D) than to the higher leaf-level factor (lower photosynthetic D; Fig. 3).

Here we interpret O'Sullivan et al.'s Earth systems model as a typical one, which means that the NPP changes it produces are common. We therefore (and sufficient for our purposes) choose the damping constant D_1 as a good estimator of the total change in NPP of the terrestrial biosphere since 1960. Hence

$$D_L \approx (815 \pm 433)ppmvy = (83 \pm 44)Pay = (2606 \pm 1383)10^6 Pas. \quad (14)$$

D_L is on the order of viscosity indicated for bitumen/asphalt (Mezger, 2006).

4.2 Estimating the Damping Constant D_O

Increasing concentrations of CO_2 in the atmosphere trigger the uptake of carbon by the oceans (National Oceanic and Atmospheric Administration, 2017). Like the uptake of carbon by the terrestrial biosphere, we consider this process to behave like a Newton (damping) element in our MB because of the irreversibility (due to hysteresis) on the shorter time scale we are interested in (Schwinger and Tjiputra, 2018).

https://doi.org/10.5194/esd-2021-27
Preprint. Discussion started: 1 July 2021

The Revelle (buffer) factor (R) quantifies how much atmospheric CO_2 can be absorbed by homogeneous reaction with seawater. R is defined as the fractional change in CO_2 relative to the fractional change in dissolved inorganic carbon (DIC):

$$R = \frac{\Delta pCO_2/pCO_2}{\Delta DIC/DIC}. \tag{15}$$

(Here, in contrast to before, atmospheric CO_2 is referred to in units of μatm and therefore indicated by pCO_2.) An R value of 10 indicates that a 10% change in atmospheric CO_2 is required to produce a 1% change in the total CO_2 content of seawater (Bates et al. 2014; Egleston et al., 2010; Emerson and Hedges, 2008).

DIC and R have been observed at seven ocean carbon time-series sites for periods from 15 to 30 years (between 1983 and 2012) to change slowly and linearly with time (Bates et al. 2014):

$$\frac{\Delta DIC}{\Delta t} \approx [0.8; 1.9]\mu molkg^{-1}y^{-1} \tag{16}$$

$$\frac{\Delta R}{\Delta t} \approx [0.01; 0.03]y^{-1} \tag{17}$$

(see also Supplementary Data 2). Here it is sufficient to proceed with spatiotemporal averages. As before, the cumulative increase in atmospheric CO_2 concentration since 1983, $\Delta pCO_2 = pCO_2(t) - pCO_2(1983)$, exhibits a moderate exponential (close to linear) trend. Thus, plotting annual changes in pCO_2, normalised on the rates of strain $\frac{(\Delta DIC/DIC)}{\Delta t}$, versus time allows the remaining (moderate) trend to be interpreted alternatively, namely, as an average oceanic damping constant with appropriate uncertainty given by half the maximal range (see Fig. 4 and Supplementary Data 2):

$$D_O \approx (3005 \pm 588)ppmvy = (304 \pm 60)Pay = (9602 \pm 1877)10^6Pas. \tag{18}$$

https://doi.org/10.5194/esd-2021-27
Preprint. Discussion started: 1 July 2021

Earth System Dynamics Discussions

D_O is on the order of viscosity indicated for bitumen/asphalt, yet approximately 3.7 times greater than D_L.

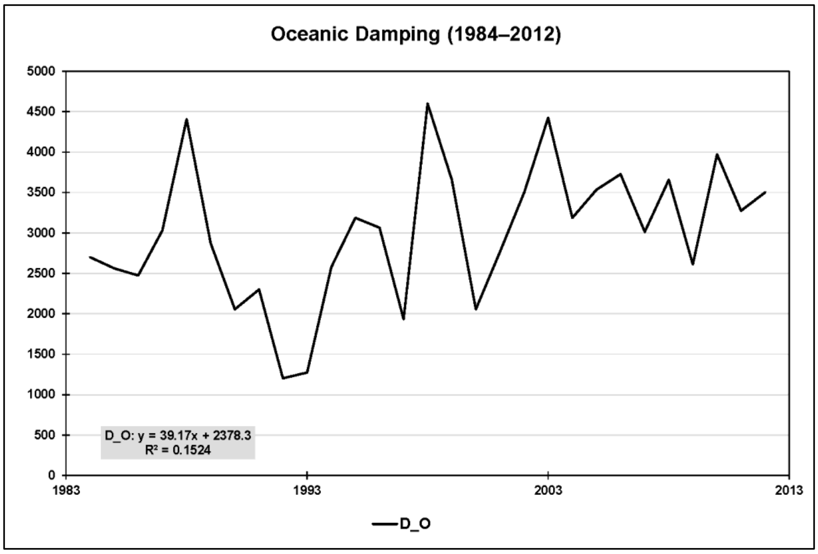

Fig. 4: Oceanic carbon uptake perceived as damping (in ppmv y) based on observations at seven ocean carbon time-series sites for periods from 15 to 30 years (between 1983 and 2012). The linear trend in oceanic damping, shown at the bottom, is used to interpret damping as a constant with appropriate uncertainty (given by half the maximal range).

4.3 Estimating the Compression Modulus *K*

The long-lasting increase in GHG emissions has caused the CO_2 concentration in the atmosphere to increase and the atmosphere as a whole to warm (with tropospheric warming outstripping stratospheric cooling) and to expand (in the troposphere by approximately 15–20 m per decade since 1990) (Global Carbon Project, 2019; Lackner et al., 2011; Philipona et al., 2018; Steiner et al., 2011; Steiner et al., 2020). Our whole-subsystem (net-warming) view does not invalidate the known facts that CO_2 in the atmosphere is well-mixed (except for very low altitudes where deviations from uniform CO_2 concentrations are caused by the dynamics of carbon sources and sinks) and that the volume percentage of CO_2 in the atmosphere stays almost constant up to high altitudes Abshire et al., 2010; Emmert et al., 2012).

Compared to the slow uptake of carbon by land and oceans, we assume the atmosphere to be represented well by a Hooke element in the MB and this to serve as a (sufficiently stable) surrogate physical descriptor for the reaction of the atmosphere as a whole (Sakazaki and Hamilton, 2020). However, in the case of a gas, Young's modulus E must be replaced by the compression modulus K, the reciprocal of which is compressibility κ. Both K and κ scale with altitude which we get to grips with in the following. Compressibility is defined by

$$\kappa = \frac{1}{K} = -\frac{1}{V}\frac{dV}{dp} \tag{19}$$

($\kappa > 0$) (OpenStax, 2020). Depending on whether the compression happens under isothermal or adiabatic conditions, the compressibility is distinguished accordingly. It is defined by

$$\kappa_{it} = \frac{1}{p} \tag{20a}$$

in the isothermal case and

$$\kappa_{ad} = \frac{1}{\gamma p} \tag{20b}$$

in the dry adiabatic case, where γ is the isentropic coefficient of expansion. Its value is 1.403 for dry air (1.310 for CO_2) under standard temperature (273.15 K) and pressure (1 atm; 101.325 kPa) (Wark, 1983). We consider a carbon-enriched atmosphere also as air.

However, the observed expansion of the troposphere happens neither isothermally nor dry-adiabatically but polytropically. Moreover, our ignorance of the exact value of κ is

https://doi.org/10.5194/esd-2021-27
Preprint. Discussion started: 1 July 2021

overshadowed by the uncertainty in altitude—or top of the atmosphere (TOA)—which we need as a reference for κ (thus K). As a matter of fact, there exists considerable confusion as to which altitude the TOA refers in climate models (CarbonBrief, 2018; NASA Earth Observatory, 2006).

To advance, we make reference to the (dry adiabatic) standard atmosphere, which assigns a temperature gradient of –6.5°C/1000 m up to the tropopause at 11 km, a constant value of –56.5°C (216.65 K) above 11 km and up to 20 km, and other gradients and constant values above 20 km (Cavcar, 2000; Mohanakumar, 2008). Guided by the distribution of atmospheric mass by altitude, we choose the stratopause as our TOA (at about 48 km altitude and 1 hPa), with uncertainty ranging from mid-to-higher stratosphere (at about 43 km altitude and 1.9 hPa) to mid-mesosphere (at about 65 km altitude and 0.1 hPa) (Digital Dutch, 1999; International Organization for Standardization, 1975; Mohanakumar, 2008; Zellner, 2011). We assign the resulting uncertainty of 90% in relative terms to

$$K = (1 \pm 0.9) hPa = (100 \pm 90) Pa, \quad (21)$$

which we consider sufficiently large to compensate for the unknown isentropic coefficient in the first place; that is, $[K_{ad,min}; K_{ad,max}] \in [K_{it,min}; K_{ad,max}] \in [K_{min}; K_{max}]$. For comparison, K_{ad} would range from 400 to 412 hPa were the TOA allocated within the troposphere (exhibiting, the reference used here, an expansion of 20 m; see Supplementary Information 8).

5. Main Findings (1837 words)

Equation (1a) (or [2a], respectively) and equation (1b) are used stepwise in combination to conduct three sets of stress-strain experiments including sensitivity experiments (SEs):

A. for the period 1959–2015 assuming zero stress and strain in 1959,

B. for the period 1959–2015 assuming zero stress and strain in 1900, and

C. for the period 1959–2015 assuming zero stress and strain in 1850.

The logic of the experiments is determined by both the availability of data (see Supplementary Information 6) and the increasing complementarity from A to C (see below). The basic procedure is always the same: We insert into equation (1a) our first-order estimates of $D_L \approx (83 \pm 44)Pay$; $D_O \approx (304 \pm 60)Pay$, that is, $D = D_L + D_O \approx (387 \pm 74)Pay$; and $K \approx (100 \pm 90)Pa$. At the same time, we use the growth factor $\alpha_{ppm} = 0.0043y^{-1}$, which reflects the exponential increase in the CO_2 concentration in the atmosphere between 1959 and 2018 (see Supplementary Data 1) as our first-order estimate for α in $\dot{\varepsilon} = \alpha\, exp(\alpha t)$, the rate of change in strain ε. We apply equation (1a) by varying both K/D and α to reproduce the known stress σ on the left, given by the CO_2 emissions from fossil fuel burning and land use. To restrict the number of variation parameters to two, we let K and D deviate from their respective mean values equally in relative terms (i.e., we assume that our first-order estimates exhibit equal inaccuracy in relative terms) and express α as a multiple of α_{ppm}. This is easily possible with the introduction of suitable factors (see Supplementary Data 3) that allow σ to be reproduced quickly and with sufficient accuracy. The main reason this works well is that the two factors pull the two exponential functions on the right side of equation (2a)—$\dot{\varepsilon}(t)$ and $\left(1 - q_\beta^t\right)$, which determine the quality of the fit—in different directions.

To A

This is our set of reference experiments, all for the period 1959–2015. This set comprises **A.1)** a stress-explicit experiment, **A.2)** three strain-explicit experiments, and **A.3)** SEs

https://doi.org/10.5194/esd-2021-27
Preprint. Discussion started: 1 July 2021

expanding the strain-explicit experiments. The parameters α, λ , and λ_β are reported in y^{-1}, as is commonly done.

To A.1: In this experiment we vary the ratio K/D (λ in Table 1) and α to reproduce the monitored stress $\sigma(t)$ on the left side of equation (2a) (see Supplementary Data 3). This tuning process (hereafter referred to as "Case 0") allows us to test whether K and D, in particular, stay within their estimated limits, namely, $K \in [10; 190]Pa$ and $D \in [313; 461]Pay$ or, equivalently, $\lambda \in [0.0217; 0.6078]y^{-1}$. Column "Case 0" in Table 1 indicates that this case is practically identical to choosing $\lambda = (10/461)y^{-1} = 0.0217y^{-1}$, the smallest ratio K/D deemed possible. For Case 0 we find $K = 9.9Pa$ and $D = 461.5Pay$ (thus, $\lambda = K/D = 0.0214y^{-1}$) and, concomitantly, $\alpha = 0.0247y^{-1}$ (thus, $\lambda_\beta = (K/D)\beta = (K/D) + \alpha = 0.0461y^{-1}$).

Table 1: Overview of parameters in experiments A.1–A.3.

Parameter		Case 0	Case 1	Case 12	Case 13	Case 2	Case 21	Case 23	Case 3	Case 31	Case 32
		stress explicit	strain explicit	sensitivity experiments Case 1		strain explicit	sensitivity experiments Case 2		strain explicit	sensitivity experiments Case 3	
K	Pa	9.9	10	10	10	100	100	100	190	190	190
D	Pa y	461.5	461	461	461	387	387	387	313	313	313
λ [a,b]	y^{-1}	0.0214	0.0217	0.0217	0.0217	0.2584	0.2584	0.2584	0.6078	0.6078	0.6078
λ^{-1}	y	46.8	46.1	46.1	46.1	3.87	3.87	3.87	1.65	1.65	1.65
α [a]	y^{-1}	0.0247	0.0248	0.0158	0.0174	0.0158	0.0248	0.0174	0.0174	0.0248	0.0158
β	1	2.158	2.144	1.729	1.803	1.061	1.096	1.067	1.029	1.041	1.026
λ_β [a]	y^{-1}	0.0461	0.0465	0.0375	0.0391	0.2742	0.2832	0.2758	0.6252	0.6236	0.6236
λ_β^{-1}	y	21.7	21.5	26.7	25.6	3.65	3.53	3.63	1.60	1.58	1.60
q_β	1	0.9549	0.9546	0.9632	0.9617	0.7602	0.7534	0.7590	0.5351	0.5312	0.5360
T_∞	1	21.19	21.02	26.19	25.10	3.17	3.05	3.15	1.15	1.13	1.16
$M_\infty = T_\infty/q_\beta$	1	22.19	22.02	27.19	26.10	4.17	4.05	4.15	2.15	2.13	2.16
$P_\infty = 1/T_\infty$	1	0.0472	0.0476	0.0382	0.0398	0.3155	0.3274	0.3176	0.8686	0.8825	0.8657
$\lambda/\lambda_\beta = 1/\beta$	%	46.3	46.6	57.8	55.5	94.2	91.2	93.7	97.2	96.1	97.5
n at $T/T_\infty = 0.5$	1	---	28	34	33	5	5	5	3	3	3

https://doi.org/10.5194/esd-2021-27
Preprint. Discussion started: 1 July 2021

Earth System Dynamics Discussions

λ / LN(M·P)	%	---	5	5	5	36	36	36	54	53	54
n at M/M_∞=0.5	1	---	15	19	18	3	2	3	1	1	1
λ/ln(M·P)	%	---	4	4	4	22	21	22	n.a.	n.a.	n.a.
n at T/T_∞=0.95	1	---	98	121	116	17	17	17	8	8	8
λ / LN(M·P)	%	---	25	28	27	82	79	81	91	90	91
n at M/M_∞=0.95	1	---	64	80	77	11	11	11	5	5	5
λ / LN(M·P)	%	---	13	13	13	61	60	61	74	74	74

[a] Given in y^{-1}.

[b] Derived for K and D deviating from their respective mean values equally in relative terms.

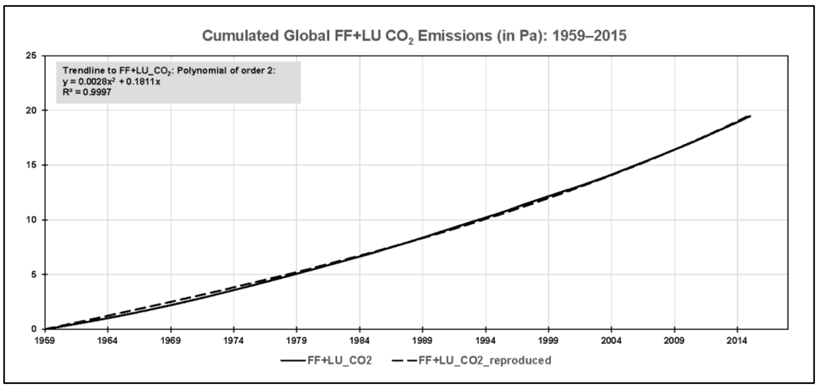

Fig. 5: Case 0: K/D and α on the right side of equation (2a) are tuned to reproduce the stress $\sigma(t)$ on the left side of that equation, given by the monitored (but cumulated) CO_2 emissions from fossil fuel burning and land use activities (in Pa).

Fig. 5 reflects the result of the tuning process graphically. It shows how well the monitored stress, given by the cumulated CO_2 emissions from fossil fuel burning and land use activities since 1959, can be reproduced by equation (2a). The quality of the tuning is observed by summing the squares of differences between monitored and reproduced stress from 1959 to 2015 using the SUMXMY2 command in Excel. (We stopped the tuning process with the sum

https://doi.org/10.5194/esd-2021-27
Preprint. Discussion started: 1 July 2021

Earth System Dynamics Discussions

at about 1.400 Pa², when changes in K and D became negligible, resulting in a correlation coefficient of 0.9998; see Supplementary Data 3.)

Fig. 5 also shows the parameters needed to describe the monitored stress by a second-order polynomial regression (see the grey box in the upper left corner of the figure). We have not yet used this regression but will do so in the strain-explicit experiments described next.

To A.2: We use equation (1b) with $\sigma(0) = \varepsilon(0) = 0$ and $\sigma(t) = 0.0028t^2 + 0.1811t$, the second-order polynomial regression of the monitored stress (cf. Fig. 5), to conduct three experiments (hereafter referred to as "Cases 1–3") to explore the spread in the strain ε. To this end, we let the ratio K/D vary from minimum (Case 1) to mean (Case 2) to maximum (Case 3; see Table 1 and Supplementary Data 4) irrespective of the outcome of the Case 0 experiment, which suggests that compared to Cases 2 and 3, Case 1 (K minimal: the atmosphere is rather compressible, D maximal: the land and oceans are rather viscous) appears to be more in conformity with reality than Cases 2 and 3.

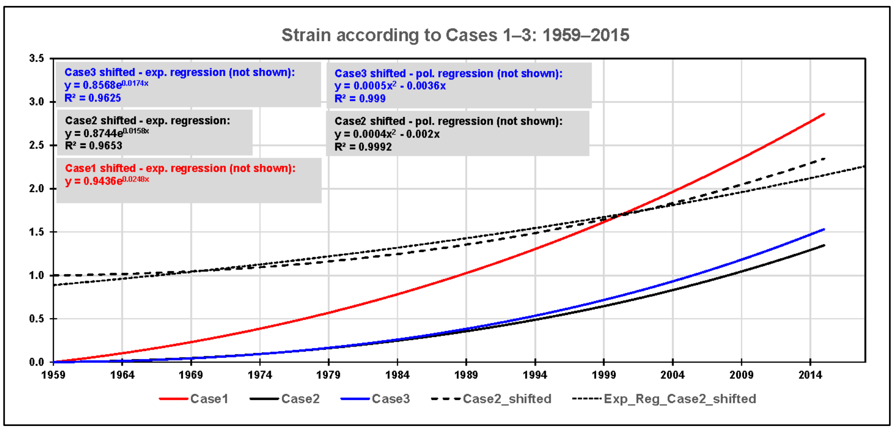

Fig. 6: Cases 1–3: The ratio K/D is varied from minimum (Case 1: solid red) to mean (Case 2: solid black) to maximum (Case 3: solid blue) to explore the spread in the strain ε

https://doi.org/10.5194/esd-2021-27
Preprint. Discussion started: 1 July 2021

(in units of 1) on the left side of equation (1b), while the monitored stress is described by a second-order polynomial (see the text). These strain responses have to be shifted upward (so that they pass through 1 in 1959) to derive their rates of change, if described by an exponential regression (here only demonstrated for Case 2). As is already illustrated in Case 0, the exponential regression in Case 1 is excellent (see the text), whereas second-order polynomial regressions provide better fits in Cases 2 and 3 (see the boxes in the figure; the polynomial regressions are not shown).

Fig. 6 reflects these experiments graphically. It shows that the range of strain responses is encompassed by Case 1 ($K/D = (10/461)y^{-1}$) and Case 2 ($K/D = (100/387)y^{-1}$), not by Case 1 and Case 3 ($K/D = (190/313)y^{-1}$)—the solid blue line (Case 3) falls in between the solid red (Case 1) and solid black (Case 2) lines—resulting from how K and D dominate the individual parts of equation (1b). These strain responses have to be shifted upward (so that they pass through 1 in 1959) to describe them by an exponential regression and to derive their rates of change. The exponential fit is excellent only in Case 1, as already illustrated in Case 0 (Case 0: $\lambda = 0.0214y^{-1}$, Case 1: $\lambda = 0.0217y^{-1}$), but inferior to the polynomial regressions, here of the second order, in Cases 2 and 3. However, a second-order polynomial approach to the strain has to be discarded because the stress derived with the help of equation (1a) would exhibit a linear behaviour with increasing time and not be a polynomial of the second order as in Fig. 6 (see Supplementary Information 9).

https://doi.org/10.5194/esd-2021-27
Preprint. Discussion started: 1 July 2021

Earth System Dynamics
Discussions

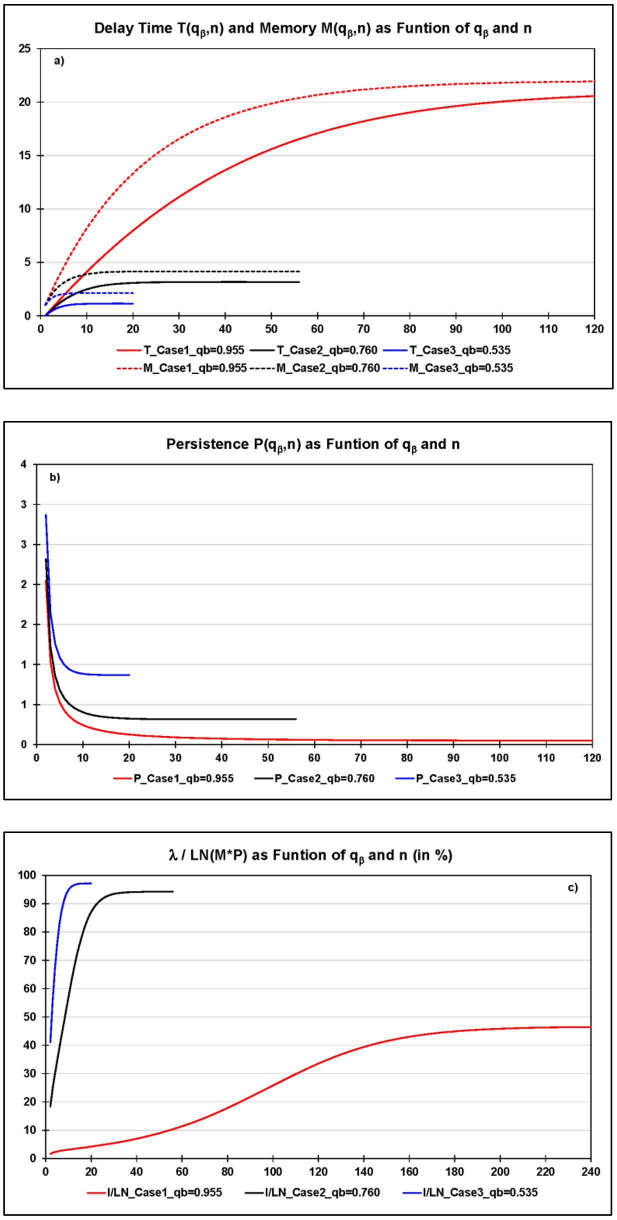

Fig. 7: Cases 1–3: **a)** delay time T and memory M (in units of 1), **b)** persistence P (in units of 1), and **c)** the ratio $\lambda/ln(M \cdot P)$ (in %); all are versus time (in units of 1).

In this regard we note that a more targeted way forward would be to use a piecemeal approach. This approach requires the data series to be sliced into shorter time intervals, during which an exponential fit for the strain (which we assume to hold in principle in deriving equation [2a] here) is sufficiently appropriate. Fortunately, as the SEs in A.3 indicate, we can hazard the consequences of using suboptimal growth factors resulting from suboptimal exponential regressions for the strain.

Equations (3) to (5) are used to determine delay time T, memory M, and persistence P (in units of 1) for Cases 1–3 as well as their characteristic limiting values T_∞, M_∞, and P_∞ (see Table 1 and Supplementary Data 5 to 8). Fig. 7a and 7b reflect the behaviour of T, M, and P over time (in units of 1). For a better overview, Table 1 lists the times when these parameters exceed 50% or 95%, respectively, of their limiting values (without indicating whether these levels go hand in hand with, e.g., global-scale ecosystem changes of equal magnitude). In the table we also specify the ratio $\lambda/ln(M \cdot P)$ for each of these times (see also Fig. 7c). The ratio approaches λ/λ_β for $n \to \infty$ and indicates (as a percentage) how much smaller the system's natural rate of change in the numerator turns out compared to the system's rate of change in the denominator under the continued increase in stress. As is illustrated, in particular, by Case 1 in the figure, the ratio does not increase at a constant pace as n increases, which shows the nonlinear strain response of the atmosphere–land/ocean system.

To A.3: Three sets of SEs serve to assess the influence of the exponential growth factor on the strain-explicit experiments described above:

SE1: $\alpha_1 = 0.0248y^{-1}$ as in Case 1 (cf. Fig. 6) is also used in Cases 2 and 3 (hereafter referred to as "Cases 21 and 31").

https://doi.org/10.5194/esd-2021-27
Preprint. Discussion started: 1 July 2021

Earth System Dynamics
Discussions

SE2: $\alpha_2 = 0.0158y^{-1}$ as in Case 2 (cf. Fig. 6) is also used in Cases 1 and 3 (hereafter referred to as "Cases 12 and 32").

SE3: $\alpha_3 = 0.0174y^{-1}$ as in Case 3 (cf. Fig. 6) is also used in Cases 1 and 2 (hereafter referred to as "Cases 13 and 23").

Table 1 shows that the influence of a change in the exponential growth factor is small vis-à-vis the dominating influence of K and D and the quality in the estimates of T, M, and P. For instance, the dimensionless time n at $M/M_\infty = 0.5$ ranges from 15 to 19 in Case 1 and Case 1–related experiments (small persistency) and from 2 to 3 in Case 2 and Case 2–related experiments (great persistency); in Case 3 and Case 3–related experiments, it does not exhibit a range at all ($n \approx 1$; very great persistency). These ranges for n tell us how long it takes to build up 50% of the memory with time running as of $n = 0$ (1959).

Table 2: Cases 1–3 and related experiments: Build-up of memory (%) as of $n = 0$ (1959).

Time		**Increase in memory as of n=0 (1959)**		
		Cases 1, 12, 13	**Cases 2, 21, 23**	**Cases 3, 31, 32**
y	**1**	**%**	**%**	**%**
1959 [a]	0	0.0	0.0	0.0
1964	5	17–21	75–76	96
1970	11	34–40	95–96	100
2015	56	88 – 93	100	---

[a] Start year: $\sigma_0 = \varepsilon_0 = 0$.

Alternatively, we can ask how much memory has been build up until a given year. Table 2 tells us that after 56 years (i.e., in 2015) memory is still building up only in Case 1 and Case 1–related experiments, which means that the system still responds in its own characteristic way (as a result of a small K and a great D) to the continuously increasing stress; this is not so in Cases 2 and 3 (and related experiments). In the latter two cases today's uptake of carbon by land and oceans happens de facto outside the system's natural regime and solely in

https://doi.org/10.5194/esd-2021-27
Preprint. Discussion started: 1 July 2021

response to the sheer, continuously increasing stress imposed on it, whereas in Case 1 and Case 1–related experiments the limits of the natural regime are not yet reached. This interpretation of Cases 1–3 (and related experiments) does not depend on how much carbon the system already took up before 1959, because M is additive and the current M/M_∞ value considers M/M_∞ to be achieved historically (e.g., during the previous time interval) by way of adjusting initial conditions.

Finally, it is important to note that it is prudent to expect that natural elements (like land and oceans) will not continue to maintain their damping capacity—or their capacity to embark on a, most likely, hysteretic downward path in the case of a sustained decrease in emissions—even well before they reach the limits of their natural regimes. They may simply collapse globally.

To B and C

We report on the sets of stress-strain experiments B and C in combination. They can be understood as a repetition of the 1959–2015 Case 0 experiment (see A.1) but with the difference that now upstream emissions as of 1900 (B) or 1850 (C), respectively, are considered. This allows initial conditions for 1959 other than zero, as in the Case 0 experiment, to be taken into account (see Supplementary Information 10 and Supplementary Data 9 to 16):

Case 0: 1959–2015
B: 1900–1958 (upstream emissions), 1959–2015
C: 1850–1958 (upstream emissions), 1959–2015

https://doi.org/10.5194/esd-2021-27
Preprint. Discussion started: 1 July 2021

The experiments can be ordered consecutively in terms of time with the three 1959–2015 periods comprising a min–max interval to facilitate the drawing of a number of robust results in spite of the uncertainty underlying these stress-strain experiments (see Supplementary Information 10). Between 1850 and 1959–2015 (i) the compression modulus K increased from ~2 to 10–13 Pa (the atmosphere became less compressible) while (ii) the damping constant D decreased from ~468 to 459–462 Pa y (the land and oceans became less viscous), with the consequence that (iii) the ratio $\lambda = K/D$ increased from ~0.004–0.005 y^{-1} to 0.021–0.028 y^{-1} (i.e., by a factor of 4–6). Likewise, (iv) delay time T_∞ decreased (hence persistence P_∞ increased) from ~51 (~0.02) to 18–21 (0.047–0.055) while (v) memory M_∞ decreased from ~52 to 19–22 on the dimensionless time scale.

6. Account of the Findings

Our Case 0 experiment (see A.1) in combination with stress-strain experiments B and C described above allows us to draw some precautionary conclusions. The values of the Case 0 parameters T_∞ and M_∞, in particular, are at the upper end of the respective 1959–2015 min–max intervals (see Supplementary Information 10). That is, the respective characteristic ratios T/T_∞ and M/M_∞ reach specified levels (e.g., 0.5 or 0.95; see Fig. 7a) slightly sooner than when T_∞ and M_∞ take on values at the lower end of the 1959–2015 min–max intervals.

Given that Case 0 is well represented by Case 1 (see A.2), we can use the parameter values of the latter. According to column “Case 1” in Table 1, M/M_∞ and T/T_∞ reached their 0.5 levels after about 15 and 28 year-equivalent units on the dimensionless time scale (which was in 1974 and 1987), whereas they will reach their 0.95 levels after about 64 and 98 year-equivalent units (which will be in 2023 and 2057) if the exponential growth factor α remains unchanged in the future. However, the increase in P_∞, here by a factor of 2–3, indicates that

https://doi.org/10.5194/esd-2021-27
Preprint. Discussion started: 1 July 2021

the atmosphere–land/ocean system is progressively trapped in terms of persistence, which means that it will become progressively more difficult to strain-relax the entire system (i.e., the atmosphere including land and oceans). A mere 1-year decrease of a few percentage points in emissions, as reported recently for 2020, will have virtually no impact Global Carbon Project, 2020).

We understand, in particular, the ability of a system to build up memory effectively as its ability to respond still in its own characteristic way (i.e., within its natural regime; see A.3). Therefore, it appears precautionary to prefer memory over delay time in avoiding potential system failures globally in the future. These we expect to happen well before 2050 if the current trend in emissions is not reversed immediately and sustainably.

We consider this statement robust given both the uncertainties we dealt with in the course of our evaluation and the restriction of our variation parameters to two. One of the two variation parameters (λ) presupposes knowing K and D with equal inaccuracy in relative terms. The introduction of this parameter, in particular, offers a great applicational benefit, but no serious restriction given that, while α is held constant, it is the K/D ratio that counts and whose ultimate value is controlled by consistency—which comes in as a powerful rectifier. As a matter of fact, fulfilling consistency results in a K/D ratio that ranges close to the lower uncertainty boundary which we deem adequate based on our preceding assessment. That is, a smaller K: the atmosphere is more compressible than previously thought; and a greater D: land and oceans are more viscous than previously thought. However, the overall effect of the continued release of GHG emissions since 1850 on the K/D ratio is unambiguous—the ratio increased by a factor 4–6 (K increased: the atmosphere became less compressible; D

https://doi.org/10.5194/esd-2021-27
Preprint. Discussion started: 1 July 2021

Earth System Dynamics
Open Access
EGU
Discussions

decreased: land and oceans became less viscous), resulting in the aforementioned changes in delay time, memory, and persistence.

The latter two Earth system characteristics can be summarized in lieu of the questions posed in the beginning: Earth's memory is a limited buffer, approximately 60% of which humankind had already exploited prior to 1959; while its persistence (path dependency) increases by approximately a factor 2–3 if the release of emissions globally continues as before.

Acknowledgements

Funding was provided by the authors' home institutions. Additional funding to facilitate collaboration between the Lviv Polytechnic National University and IIASA was provided by the bilateral Agreement on Scientific and Technological Co-operation between the Cabinet of Ministers of Ukraine and the Government of the Republic of Austria (S&T Cooperation Project 10/2019; https://oead.at/en/ and www.mon.gov.ua/). Net primary production, land-use change emission, and atmospheric expansion data were kindly provided personally by Michael O'Sullivan (University of Exeter), Julia Pongratz (Ludwig Maximilian University of Munich), and Andrea K. Steiner (Wegener Center for Climate and Global Change, Graz).

Data Availability

Supplementary Material (Supplementary Information and Supplementary Data): https://doi.org/10.22022/em/06-2021.123

Author Contributions

M.J. set up the physical model of the atmosphere–land/ocean system; derived its delay time, memory, and persistence; and provided the initial estimates of its compression and damping characteristics. R. B. contributed to the physical and mathematical improvement of the method and the physical consistency of results. I. R. and P. Z. contributed to the inspection of mathematical relations globally and their generalizations. P.Z. contributed to the strengthening of the method by evaluating alternative memory concepts known in mathematics.

https://doi.org/10.5194/esd-2021-27
Preprint. Discussion started: 1 July 2021

Earth System Dynamics
Discussions

References

Abshire, J. B., Riris, H., Allan, G. R., Weaver, C. J., Mao, J., Sun, X., Hasselbrack, W. E., Kawa, S. R. and Biraud, S. Pulsed airborne lidar measurements of atmospheric CO_2 column absorption. *Tellus B* **62**(5), 770–783 (2010). https://doi.org/10.1111/j.1600-0889.2010.00502.x

Aghabozorgi, S., Shirkhorshidi, A. S. and Wah, T. Y. Time-series clustering – a decade review. *Inform. Syst.* **53**, 16–38 (2015). https://doi.org/10.1016/j.is.2015.04.007

Amthor, J. S. and Koch, G. W. Biota growth factor β: stimulation of terrestrial ecosystem net primary production by elevated atmospheric CO_2. In: *Carbon Dioxide and Terrestrial Ecosystems.* (eds Koch, G. W. & Mooney, H. A.), 399–414 (Academic Press, Inc., 1996).

Barros, C.P., Gil-Alana, L.A. and Perez de Gracia, F. Stationarity and long range dependence of carbon dioxide emissions: evidence for disaggregated data. *Environ. Resource Econ.* **63,** 45–56 (2016). https://doi.org/10.1007/s10640-014-9835-3

Bates, N. R., Astor, Y. M., Church, M. J., Currie, K., Dore, J. E., González-Dávila, M., Lorenzoni, L., Muller-Karger, F., Olafsson, J. and Santana-Casiano, J. M. A Time-series view of changing ocean chemistry due to ocean uptake of anthropogenic CO_2 and ocean acidification. *Oceanography* **27**, 126–141 (2014). https://doi.org/10.5670/oceanog.2014.16

Belbute, J. M. and Pereira, A. M. Do global CO_2 emissions from fossil-fuel consumption exhibit long memory? A fractional integration analysis. *Appl. Econ.*, 4055–4070 (2017). https://doi.org/10.1080/00036846.2016.1273508

Bertram, A. and Glüge, R. *Festkörpermechanik: Einachsige Materialtheorie: Viskoelastizität: Der MAXWELL-Körper* (Otto-von-Guericke University Magdeburg, Germany, 2015). https://docplayer.org/11977674-Festkoerpermechanik-mit-beispielen-von-albrecht-bertram-von-rainer-gluege-otto-von-guericke-universitaet-magdeburg.html

https://doi.org/10.5194/esd-2021-27
Preprint. Discussion started: 1 July 2021

Boucher, O., Halloran, P. R., Burke, E. J., Doutriaux-Boucher, M., Jones, C. D., Lowe, J., Ringer, M. A., Robertson, E. and Wu, P. Reversibility in an Earth system model in response to CO_2 concentration changes. *Environ. Res. Lett.* 7, 24013 (9pp) (2012). https://doi.org/10.1088/1748-9326/7/2/024013

Caballero, R., Jewson, S. and Brix, A. Long memory in surface air temperature: Detection, modeling, and application to weather derivative valuation. *Clim. Res.* **21**, 127–140 (2002). https://doi.org/10.3354/cr021127

CarbonBrief. Climate modelling. Q&A: How do climate models work? (15 January 2018). https://www.carbonbrief.org/qa-how-do-climate-models-work (last access 24 June 2021)

Cavcar, M. The international standard atmosphere (ISA). Anadolu University, Turkey (7pp) (2000). http://fisicaatmo.at.fcen.uba.ar/practicas/ISAweb.pdf

Darlington, R. B. A regression approach to time-series analysis. Script (Cornell University 1996). http://node101.psych.cornell.edu/Darlington/series/series0.htm

Darlington, R. B. and Hayes, A. F. Regression analysis and linear models: Concepts, Applications, and Implementation. (Guilford Publications Inc., 2016). https://www.guilford.com/books/Regression-Analysis-and-Linear-Models/Darlington-Hayes/9781462521135

Digital Dutch. 1976 Standard atmosphere calculator. (1999). https://www.digitaldutch.com/atmoscalc/ (last access 24 June 2021)

Dusza, Y., Sanchez-Cañete, E. P., Le Galliard, J.-F., Ferrière, R., Chollet, S., Massol, F., Hansart, A., Juarez, S., Dontsova, K., van Haren, J., Troch, P., Pavao-Zuckerman, M. A., Hamerlynck, E. and Barron-Gafford, G. A. Biotic soil-plant interaction processes explain most of hysteric soil CO_2 efflux response to temperature in cross-factorial mesocosm experiment. *Sci. Rep.* **10,** 905 (11pp) (2020). https://doi.org/10.1038/s41598-019-55390-6

Egleston, E. S., Sabine, C. L. and Morel, F. M. M. Revelle revisited: buffer factors that quantify the response of ocean chemistry to changes in DIC and alkalinity. *Glob. Biochem. Cycles* **24,** GB1002 (9pp) (2010). https://doi.org/10.1029/2008GB003407

Emerson, S. and Hedges, J. *Chemical Oceanography and the Marine Carbon Cycle* (Cambridge University Press, 2008). https://slideplayer.com/slide/9820843/ (PDF overview of Section 4.4 by Ford, C. Lecture 10: Ocean Carbonate Chemistry: Ocean Distributions)

Emmert, J. T., Stevens, M. H., Bernath, P. F., Drob, D. P. and Boone, C. D. Observations of increasing carbon dioxide concentration in Earth's thermosphere. *Nat. Geosci.* **5**, 868–871(2012). https://www.nature.com/articles/ngeo1626 (Background source to https://phys.org/news/2012-11-atmospheric-co2-space-junk.html; last access 24 June 2021)

Flato, G., Marotzke, J., Abiodun, B., Braconnot, P., Chou, S. C., Collins, W., Cox, P., Driouech, F., Emori, S., Eyring, V., Forest, C., Gleckler, P., Guilyardi, E., Jakob, C., Kattsov, V., Reason, C. and Rummukainen, M. Evaluation of climate models. In: *Climate Change 2013: The Physical Science Basis. Contribution of Working Group I to the Fifth Assessment Report of the Intergovernmental Panel on Climate Change* ([eds. Stocker, T. F., et al.), 741–866 (Cambridge University Press, 2013). https://www.ipcc.ch/site/assets/uploads/2018/02/WG1AR5_Chapter09_FINAL.pdf

Franzke C. Long-range dependence and climate noise characteristics of Antarctic temperature data. J. *Climate* **23**(22), 6074–6081 (2010). https://doi.org/10.1175/2010JCLI3654.1

Garbe, J., Albrecht, T., Levermann, A., Donges, J. F. and Winkelmann, R. The hysteresis of the Antarctic ice sheet. *Nature* **585,** 538–544 (2020). https://doi.org/10.1038/s41586-020-2727-5

Global Carbon Project. Global carbon budget 2019. (Published on 4 December 2019, along with other original peer-reviewed papers and data sources). https://www.icos-cp.eu/science-and-impact/global-carbon-budget/2019

Global Carbon Project. Carbon budget 2020. (Published on 11 December 2020, along with other original peer-reviewed papers and data sources). https://www.globalcarbonproject.org/carbonbudget/index.htm

Harman, I. N. and Trudinger, C. M. The simple carbon-climate model: SCCM7. CAWCR Technical Report No. 069 (2014). https://www.cawcr.gov.au/technical-reports/CTR_069.pdf

Heimann, M. and Reichstein, M. Terrestrial ecosystem carbon dynamics and climate feedbacks. *Nature* **451,** 289–292 (2008). https://doi.org/10.1038/nature06591

International Organization for Standardization. Standard atmosphere. ISO 2533:1975 (1975). (Background source to https://en.wikipedia.org/wiki/International_Standard_Atmosphere; last access: 24 June 2021)

Lackner, B. C., Steiner, A. K., Hegerl, G. C. and Kirchengast, G. Atmospheric climate change detection by radio occultation using a fingerprinting method. *J. Climate* **24,** 5275–5291 (2011). https://doi.org/10.1175/2011JCLI3966.1

Lüdecke H. J., Hempelmann, A. and Weiss, C.O. Multi-periodic climate dynamics: spectral analysis of long-term instrumental and proxy temperature records. *Clim. Past* **9**, 447–452 (2013). https://doi.org/10.5194/cp-9-447-2013

Luo, Y. and Mooney, H. A. Stimulation of global photosynthetic carbon influx by an increase in atmospheric carbon dioxide concentration. In: *Carbon Dioxide and Terrestrial Ecosystems.* (eds Koch, G. W. & Mooney, H. A.), 381–397 (Academic Press, 1996).

Mezger, T. G. *The Rheology Handbook* (Vincentz Network, Germany, 2006). https://www.researchgate.net/profile/Abdelkader-Bouaziz/post/Technical-standard-for-

https://doi.org/10.5194/esd-2021-27
Preprint. Discussion started: 1 July 2021

the-determination-of-resin-viscosity/attachment/5c180653cfe4a7645509c278/AS%3A704923863900166%401545078354412/download/The+Rheology+Handbook+-+For+Users+of+Rotationa.pdf (Background source to https://de.wikipedia.org/wiki/Viskosität; last access 23 June 2021)

Mohanakumar, K. Structure and composition of the lower and middle atmosphere. In: *Stratosphere Troposphere Interactions*. 1–53 (Springer, 2008). https://doi.org/10.1007/978-1-4020-8217-7_1

Müller, G. Generalized Maxwell bodies and estimates of mantle viscosity. *Geophys. J. Int.* **87**(3), 1113–1141 (1986). https://doi.org/10.1111/j.1365-246X.1986.tb01986.x

NASA Earth Observatory. The top of the atmosphere. (20 July 2006). https://earthobservatory.nasa.gov/images/7373/the-top-of-the-atmosphere (last access 24 June 2021)

National Oceanic and Atmospheric Administration. Science on a sphere: ocean-atmosphere CO_2 exchange. NOAA Global Systems Division, Boulder CO, United States of America (2017). https://sos.noaa.gov/datasets/ocean-atmosphere-co2-exchange/ (last access 24 June 2021)

OpenStax. Stress, strain, and elastic modulus (Part 2) (5 November 2020). https://phys.libretexts.org/@go/page/6472 (last access 24 June 2021)

O'Sullivan, M., Spracklen, D. V., Batterman, S. A., Arnold, S. R., Gloor, M. and Buermann, W. Have synergies between nitrogen deposition and atmospheric CO_2 driven the recent enhancement of the terrestrial carbon sink? *Global Biogeochem. Cycles* **33,** 163–180 (2019). https://doi.org/10.1029/2018GB005922

Philipona, R., Mears, C., Fujiwara, M., Jeannet, P., Thorne, P., Bodeker, G., Haimberger, L., Hervo, M., Popp, C., Romanens, G., Steinbrecht, W., Stübi, R. and Van Malderen, R. Radiosondes show that after decades of cooling, the lower stratosphere is now warming.

https://doi.org/10.5194/esd-2021-27
Preprint. Discussion started: 1 July 2021

J. Geophys. Res. Atmos. **123**, 12,509–12,522 (2018). https://doi.org/10.1029/2018JD028901

Roylance, D. Engineering viscoelasticity (Massachusetts Institute of Technology, 2001). http://web.mit.edu/course/3/3.11/www/modules/visco.pdf

Sakazaki, S. and Hamilton, K. An array of ringing global free modes discovered in tropical surface pressure data. *J. Atmos. Sci.* **77,** 2519–2530 (2020). https://doi.org/10.1175/JAS-D-20-0053.1 (Background source to https://physicsworld.com/a/earths-atmosphere-rings-like-a-giant-bell-say-researchers/; last access 24 June 2021)

Schwinger, J. and Tjiputra, J. Ocean carbon cycle feedbacks under negative emissions. *Geophys. Res. Lett.* **45,** 5062–5070 (2018). https://doi.org/10.1029/2018GL077790

Smith, P. Soils and climate change. *Curr. Opin. Environ. Sust.* **4,** 539–544 (2012). https://doi.org/10.1016/j.cosust.2012.06.005

Steiner, A. K., Lackner, B. C., Ladstädter, F., Scherllin-Pirscher, B., Foelsche, U. and Kirchengast, G. GPS radio occultation for climate monitoring and change detection. *Radio Sci.* **46,** RS0D24 (17pp) (2011). https://doi.org/10.1029/2010RS004614

Steiner, A. K., Ladstädter, F., Randel, W. J., Maycock, A. C., Fu, Q., Claud, C., Gleisner, H., Haimberger, L., Ho, S.-P., Keckhut, P., Leblanc, T., Mears, C., Polvani, L. M., Santer, B. D., Schmidt, T., Sofieva, V., Wing, R. and Zou, C.-Z. Observed temperature changes in the troposphere and stratosphere from 1979 to 2018. *J. Climate* **33**, 8165–8194 (2020). https://doi.org/10.1175/JCLI-D-19-0998.1

Steffen, W., Richardson, K., Rockström, J., Cornell, S. E., Fetzer, I., Bennett, E. M., Biggs, R., Carpenter, S. R., de Vries, W., de Wit, C. A., Folke, C., Gerten, D., Heinke, J., Mace, G. M., Persson, L. M., Ramanathan, V., Reyers, B. and Sörlin, S. Planetary boundaries: guiding human development on a changing planet. *Science* 347, 1259855 (2015). https://science.sciencemag.org/content/347/6223/1259855

Steffen, W., Sanderson, A., Tyson, P., Jäger, J., Matson, P., Moore, B. III, Oldfield, F., Richardson, K. Schellnhuber, H. J., Turner, B. L. II and Wasson, R. J. *Global Change and the Earth System. A Planet Under Pressure.* (Springer-Verlag, 2004). http://www.igbp.net/publications/igbpbookseries/igbpbookseries/globalchangeandtheearthsystem2004.5.1b8ae20512db692f2a680007462.html

TU Delft. Rheometer. Faculty of Civil Engineering and Geosciences. The Netherlands. https://www.tudelft.nl/en/ceg/about-faculty/departments/watermanagement/research/waterlab/equipment/rheometer (last access 23 June 2021)

United Nations. Paris Agreement. Knowledge Platform (United Nations, 2015a). https://unfccc.int/process-and-meetings/the-paris-agreement/the-paris-agreement (last access 23 June 2021)

United Nations. Sustainable Development Goals. The Sustainable Development Agenda. Knowledge Platform (United Nations, 2015b). https://www.un.org/sustainabledevelopment/development-agenda/ (last access 23 June 2021)

Wark, K. *Thermodynamics* (McGraw2Hill, 1983) (Background source to http://homepages.wmich.edu/~cho/ME432/Appendix1_SIunits.pdf; cf. also https://en.wikipedia.org/wiki/Heat_capacity_ratio; last access 24 June 2021

Whitehouse, P. L., Gomez, N. King, M. A. and Wiens, D. A. Solid Earth change and the evolution of the Antarctic Ice Sheet. *Nat. Commun.* **10**, 503 (14pp) (2019). https://doi.org/10.1038/s41467-018-08068-y

Wullschleger, S. D., Post, W. M. and King, A. W. On the potential for a CO_2 fertilization effect in forests: estimates of the biotic growth factor based on 58 controlled-exposure studies. In: *Biotic Feedbacks in the Global Climatic System.* (eds Woodwell, G. M. &

Mackenzie, F. T.), 85–107 (Oxford University Press, 1995). Cf. also https://agris.fao.org/agris-search/search.do?recordID=US19950098925

Yuen, D. A., Sabadini, R. C. A., Gasperini, P. and Bischi, E. On transient rheology and glacial isostasy. *J. Geophys. Res.* **91**(Bll), 11,420–11,438 (1986). https://doi.org/10.1029/JB091iB11p11420

Zellner, R. Die Atmosphäre – Zwischen Erde und Weltall: Unsere lebenswichtige Schutzhülle. In: *Chemie über den Wolken … und darunter*. (eds Zellner, R. &Gesellschaft Deutscher Chemiker e.V.), 8–17 (Wiley-VCH Verlag GmbH & Co. KGaA, 2011). https://application.wiley-vch.de/books/sample/3527326510_c01.pdf